



HAL
open science

High frequency ion sound waves associated with Langmuir waves in type III radio burst source regions

G. Thejappa, R. J. Macdowall

► **To cite this version:**

G. Thejappa, R. J. Macdowall. High frequency ion sound waves associated with Langmuir waves in type III radio burst source regions. *Nonlinear Processes in Geophysics*, 2004, 11 (3), pp.411-420. hal-00302358

HAL Id: hal-00302358

<https://hal.science/hal-00302358>

Submitted on 18 Jun 2008

HAL is a multi-disciplinary open access archive for the deposit and dissemination of scientific research documents, whether they are published or not. The documents may come from teaching and research institutions in France or abroad, or from public or private research centers.

L'archive ouverte pluridisciplinaire **HAL**, est destinée au dépôt et à la diffusion de documents scientifiques de niveau recherche, publiés ou non, émanant des établissements d'enseignement et de recherche français ou étrangers, des laboratoires publics ou privés.

High frequency ion sound waves associated with Langmuir waves in type III radio burst source regions

G. Thejappa¹ and R. J. MacDowall²

¹Department of Astronomy, University of Maryland, College Park, MD 20742, USA

²NASA, Goddard Space Flight Center, Greenbelt, MD 20771, USA

Received: 21 August 2003 – Revised: 6 August 2004 – Accepted: 7 September 2004 – Published: 21 September 2004

Abstract. Short wavelength ion sound waves (2–4 kHz) are detected in association with the Langmuir waves (~15–30 kHz) in the source regions of several local type III radio bursts. They are most probably not due to any resonant wave-wave interactions such as the electrostatic decay instability because their wavelengths are much shorter than those of Langmuir waves. The Langmuir waves occur as coherent field structures with peak intensities exceeding the Langmuir collapse thresholds. Their scale sizes are of the order of the wavelength of an ion sound wave. These Langmuir wave field characteristics indicate that the observed short wavelength ion sound waves are most probably generated during the thermalization of the burnt-out cavitons left behind by the Langmuir collapse. Moreover, the peak intensities of the observed short wavelength ion sound waves are comparable to the expected intensities of those ion sound waves radiated by the burnt-out cavitons. However, the speeds of the electron beams derived from the frequency drift of type III radio bursts are too slow to satisfy the needed adiabatic ion approximation. Therefore, some non-linear process such as the induced scattering on thermal ions most probably pumps the beam excited Langmuir waves towards the lower wavenumbers, where the adiabatic ion approximation is justified.

The nonlinear process of self-focusing is known to generate the regions of wave concentration with spatial scales of one to several Langmuir wavelengths. The fast envelope sampler (FES) of the Unified Radio and Plasma Wave (URAP) experiment (Stone et al., 1992) on Ulysses captured coherent Langmuir wave field structures associated with several local type III radio bursts generated in the vicinity of the spacecraft. The characteristic features of these coherent field structures are the high intensities and short time scales of 15 to 90 milliseconds (6–27 km); the FES time resolution is typically 1 ms. Thejappa et al. (1999) show that (1) the normalized peak energy densities of some of these structures are $\sim 10^{-5}$; these energy densities are well above the modulational instability threshold of $\sim 10^{-8}$, (2) the 0.2-power widths of these wave packets are of 1 to 5 Langmuir wavelengths consistent with oscillating or envelope solitons, and (3) these widths correlate inversely with the peak amplitudes as expected of the 1D envelope solitons.

The plasma is pushed out from the regions of wave concentration under the action of pondermotive force, forming density cavities with initial sizes of a few Langmuir wavelengths. These density cavities cause an increase in the Langmuir wave field intensities leading to further shrinkage. The feedback between the Langmuir wave intensity and spatial scale of the density cavity continues until the width of the cavity reaches the size of ~ 20 Debye lengths λ_D . At these spatial scales, a strong Landau damping suddenly sets in causing an abrupt absorption of the Langmuir wave fields by the background electrons. This Langmuir collapse process leads to the formation of high energy tails in the electron distribution function (Pelletier, 1982), leaving behind the unstable empty density cavities. The Langmuir collapse also heats the plasma electrons creating a favorable condition $T_e > T_i$ for the accumulation of ion sound waves, where T_e and T_i are the electron and ion temperatures, respectively. The electron beams accelerated during the Langmuir collapse have been observed in several laboratory experiments (Burmasov et al., 1997). The ion sound waves radiated by the burnt-out cavitons have also been observed in experimental settings (Karfi-

1 Introduction

The electron beams accelerated during solar flares generate intense Langmuir waves in a very narrow band around the local electron plasma frequency f_{pe} while propagating from the inner corona to several AU in the interplanetary medium. The intensities of these waves fluctuate in a wide range (Kellogg et al., 1992a,b; Lin et al., 1986; Reiner et al., 1992; Gurnett et al., 1993; Thejappa et al., 1993, 1995). The in situ observations indicate that these waves are excited by the bump-on-tail distributions of energetic electrons (Lin et al., 1986).

Correspondence to: G. Thejappa
(golla@urap.gsfc.nasa.gov)

dov et al., 1990; Karfidov and Lukina, 1997; McFarland and Wong, 1997; Vyacheslavov et al., 2002) as well as in numerical simulations (Degtyarev et al., 1980).

Strong turbulence features of Langmuir wave packets were identified in the Jovian foreshock regions (Gurnett et al., 1981; Thiessen and Kellogg, 1993) as well as in type III radio burst source regions (Kellogg et al., 1992a; Thejappa et al., 1993, 1996; Thejappa and MacDowall, 1998; Thejappa et al., 1999). These features include (1) small scale sizes (\sim a few tens of Debye lengths) of the wave packets, and (2) peak intensities, which are well above the modulational instability thresholds. Other signatures of Langmuir collapse, such as the high energy electron tails or short wavelength ion-sound waves have never been identified in the interplanetary medium. In this paper, we report the first observational evidence for such short wavelength ion sound waves associated with coherent Langmuir wave field structures in the source regions of local type III radio bursts. It is important to note that the present day particle detectors can not resolve the density cavities created by the intense field structures.

We have identified 12 local type III events with intense Langmuir wave activity from March to June of 2001 in the URAP data. High frequency ion sound waves are observed during the Langmuir waves in the source regions of five of these local events. The temporal coincidence of high frequency ion sound and Langmuir waves can not be interpreted in terms of any resonant wave-wave interactions, such as the electrostatic or electromagnetic decay instabilities because of the large difference in the wavelengths of these two kinds of waves. For example, in the interplanetary medium, the electron beams with speeds of $v_b \sim 3 \times 10^9 \text{ cm s}^{-1}$ excite Langmuir waves with wavenumbers $k_L \sim 10^{-5} \text{ cm}^{-1}$, whereas the measured wavenumbers of the 2–4 kHz ion sound waves k_s are $\sim 10^{-4} \text{ cm}^{-1}$; the electrostatic and electromagnetic decay instabilities require the wavelengths of Langmuir and ion sound waves to be comparable to each other. On the other hand, the spatial scales of the coherent Langmuir wave field structures are comparable to the wavelengths of the ion sound waves. This indicates that the burnt-out cavitons left behind by the Langmuir collapse processes are probably responsible for these ion sound waves as suggested by Galeev et al. (1976). However, the direct Langmuir collapse requires very high speeds of electron beams responsible for the Langmuir waves. In the present case, some nonlinear process other than the electrostatic decay instability is probably pumping the Langmuir waves to lower wavenumbers. The most likely mechanism is the induced scattering of Langmuir waves off thermal ions.

The occurrences of long wavelength ion sound waves ($f \sim 100\text{--}200 \text{ Hz}$) in association with Langmuir waves in type III burst source regions were reported by several authors (Lin et al., 1986; Thejappa and MacDowall, 1998; Thejappa et al., 1999, 2003). These observations were interpreted in terms of electrostatic or electromagnetic decay instabilities, since (1) the wavelengths of these low frequency ion sound waves were comparable to those of Langmuir waves, and (2) the peak intensities of the Langmuir waves were well above

the electrostatic decay instability thresholds. The low frequency electromagnetic waves, identified either as whistlers or electromagnetic lower hybrid waves were also observed during Langmuir waves in the source regions of several type III bursts (Kellogg et al., 1992b; Thejappa et al., 1995). A unique type III event was studied by Thejappa and MacDowall (1998), where two types of low frequency waves, namely, long wavelength ion sound waves and whistlers were observed in association with strongly turbulent Langmuir waves. The observations of high frequency ion sound waves in association with type III burst related Langmuir waves have been reported for the first time in this paper.

Kellogg et al. (1999) reported very interesting high time resolution observations of Langmuir waves in the Earth's foreshock region. In our opinion, the events presented by these authors represent some of the best examples of 1-dimensional stable Langmuir envelope solitons because (1) they show inverse relationship between the amplitude and width consistent with Langmuir solitons (see, for similar relationship Thejappa et al., 1999), and (2) their intensities are well above the modulational instability thresholds. The high frequency ion sound waves observed during one of their high resolution Langmuir wave packets are very similar to the observations presented in this paper.

Nonlinear processes associated with Langmuir waves, especially strong turbulence processes are the focus of numerous theoretical studies (Zakharov, 1972; Goldman, 1984; Robinson, 1997), computer simulations (Nicholson et al., 1978; Degtyarev et al., 1980; Doolen et al., 1985; DuBois et al., 1993) and experimental investigations (Cheung and Wong, 1985). The intense interest in this topic is not only because of the fundamental nature of the problem (Zakharov, 1972), but also because of its practical importance in laser heating of pellets (Montgomery et al., 1999), ionospheric modification experiments (DuBois et al., 1993), solar radio astronomy (Papadopoulos et al., 1974; Smith et al., 1979; Goldstein et al., 1979; Goldman and Nicholson, 1978; Nicholson et al., 1978) and other astrophysical applications (Pelletier et al., 1988). For example, in the case of solar type III radio bursts, Langmuir collapse and related nonlinear processes are believed to play an important role in stabilization of the electron beams, and the conversion of Langmuir waves into the fundamental and second harmonic radio waves. In Sect. 2, we present the observations, in Sect. 3, we present the discussion and in Sect. 4, we present the conclusions.

2 Observations

We have identified 12 local type III bursts with intense Langmuir wave activity from March to June 2001 in the Ulysses/URAP wave data. These are at 09:02:45, 12:05:30 and 28:23:40 in March, 27:07:00 and 29:09:55 in April, 1:15:30, 6:20:30, 7:09:00 and 19:11:00 in May, and 9:21:50, 15:15:35 and 26:20:50 in June 2001. For five events, high frequency (2–4 kHz) ion sound waves were observed during Langmuir waves.

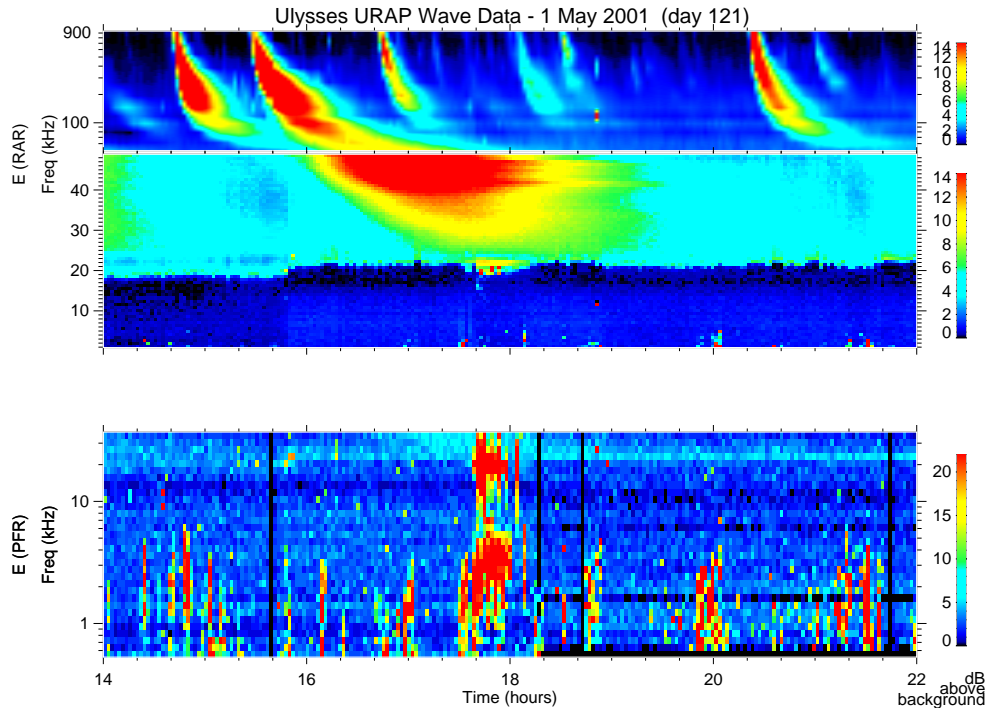


Fig. 1. The Ulysses/URAP observations of a local type III radio burst and its associated in situ waves. The top and bottom panels correspond to the radio astronomy receiver (RAR) and the plasma frequency receiver (PFR), respectively. The fast drifting emission feature from 900 kHz down to local electron plasma frequency of $f_{pe} \sim 20$ kHz is the local type III burst, the red patches at ~ 20 kHz in upper as well as lower panels are Langmuir waves and the irregular wave activity in the 1 to 4 kHz range corresponds to the short wavelength ion sound waves. The ion sound signals in the 2–4 kHz range are clearly seen during the intervals of Langmuir wave activity in the bottom panel.

Figure 1 presents the dynamic spectrum of one of the best examples. The top and bottom panels are the observations obtained by the Radio Astronomy Receiver (RAR) and the Plasma Frequency Receiver (PFR), respectively. The RAR is a high sensitivity swept frequency receiver, specifically designed to detect faint signals such as interplanetary type II and type III radio bursts. The continuous but often irregular, narrow emission band extending across the middle of the dynamic spectrum in the top panel is the quasi-thermal noise “plasma line” (Meyer-Vernet and Perche, 1989; Stone et al., 1992). The plasma line is usually used to determine the local electron density, n_e . The type III burst (16:00 to 19:00 UT) which extends all the way down to the plasma line at f_{pe} (where the Langmuir waves are clearly visible as red patches) is probably excited very close to the spacecraft. For example, Thejappa et al. (1993, 1996) have used the in situ wave observations of such local events to verify the mechanisms responsible for conversion of Langmuir waves into escaping radiation at f_{pe} and $2f_{pe}$. The PFR is characterized by a larger dynamic range and higher time resolution. Specifically, it is designed to measure the intense electrostatic signals such as the Langmuir waves and ion sound waves. The temporal coincidence of (2–4 kHz) ion sound waves and Langmuir waves is much clearer in the PFR data (bottom panel) than in the RAR data (top panel),

Figure 2 presents the time profiles of the type III burst at ~ 21.5 kHz, Langmuir waves at ~ 15.8 kHz and the high frequency ion sound waves at ~ 3.2 kHz. These time profiles clearly show the temporal coincidence of Langmuir and ion sound waves.

Figure 3 presents the average spectra of the electric field signals obtained by the PFR in the interval 17:45:04–17:54:56 UT. The peaks corresponding to the Langmuir waves at ~ 19 kHz and high frequency ion sound waves in the frequency range (2–4 kHz) occurring during this interval are clearly visible in this spectral plot.

Although a variety of waves routinely occur in the solar wind, a close temporal coincidence of low frequency waves, such as long wavelength ion sound waves or whistlers with Langmuir waves is a good indication that they are linked by some nonlinear process. In the present case, the temporal coincidence of high frequency ion sound waves and intense Langmuir waves is evident not only from the time profiles but also from the spectral plots. Such temporal coincidence is observed during several type III events. At present time, we do not know how to separate these ion sound waves from the routinely occurring waves. It is worth noting that there can be a time lag between the intense Langmuir wave peaks and ion acoustic like waves if they occur soon after the complete absorption of Langmuir waves by the background electrons.

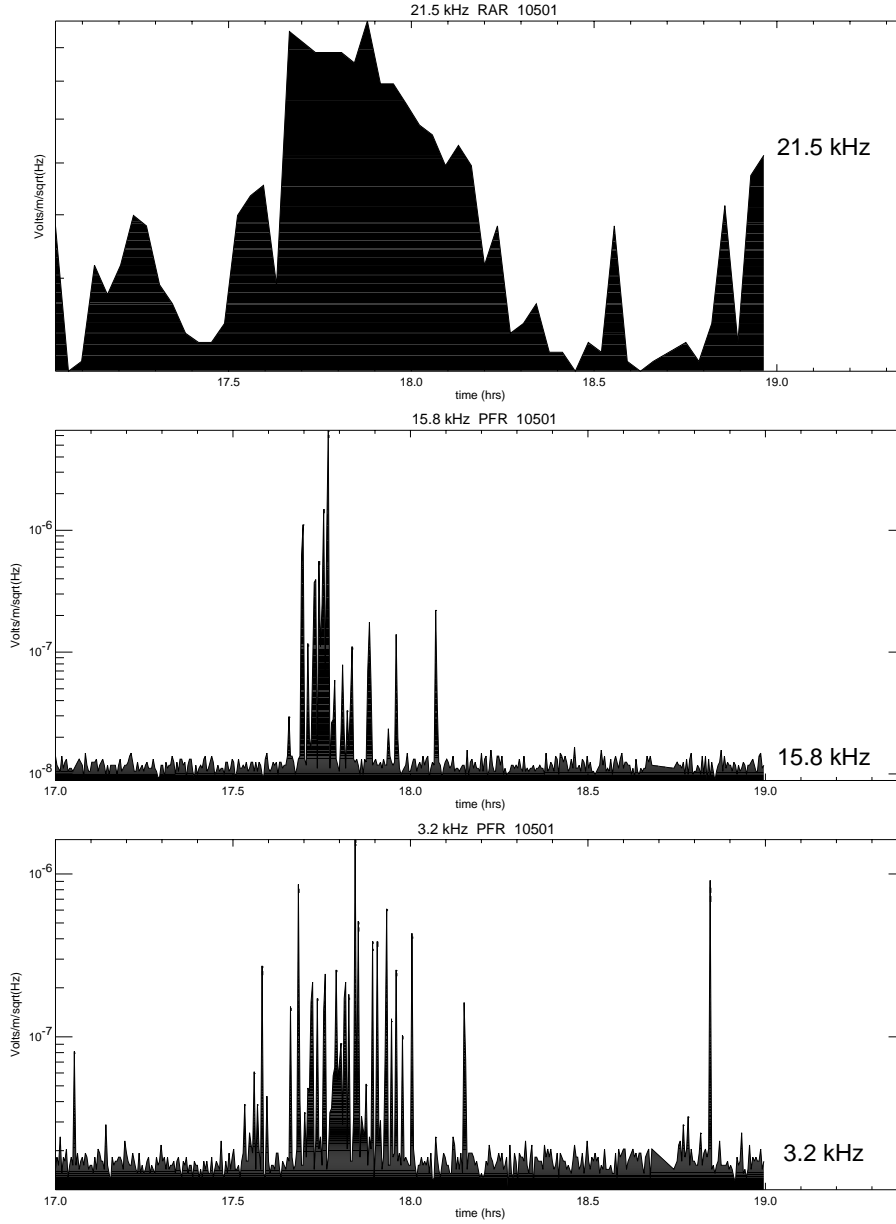


Fig. 2. Time profiles of the local type III radio burst and its associated in situ waves. The top panel showing the type III radio burst is the RAR data. The bottom two panels are from the PFR. The signals at 15.8 kHz are of Langmuir waves, whereas those of 3.2 kHz are of high frequency ion sound waves.

The frequency of ion sound waves in the spacecraft frame is

$$f_s = \frac{k_s v_s + k_s v_{sw} \cos \theta_{kv}}{2\pi}, \quad (1)$$

where k_s and v_s are the wave number and speed of the ion sound waves, respectively, v_{sw} is the solar wind speed, and θ_{kv} is the angle between the wave vector and the solar wind velocity. The first and second terms correspond to the intrinsic frequency of ion sound waves and the Doppler shift caused by the motion of the solar wind, respectively. Since

for short wavelength ion sound waves, $k_s v_s \ll k_s v_{sw}$, one can approximate

$$f_s \simeq \frac{k_s v_{sw} \cos \theta_{kv}}{2\pi}, \quad (2)$$

wavelengths $\lambda_s \simeq v_{sw}/f_s \simeq 15\lambda_D \simeq 200$ m and $k_s = 3.4 \times 10^{-2} \text{ m}^{-1}$ for $\cos \theta_{kv} \sim 1$, $f_s \simeq 2$ kHz, $v_{sw} \simeq 365 \text{ km s}^{-1}$, and Debye length $\lambda_D \sim 13.6$ m. The solar wind velocity v_{sw} is obtained from the Ulysses SWOOPS instrument (Bame et al., 1992).

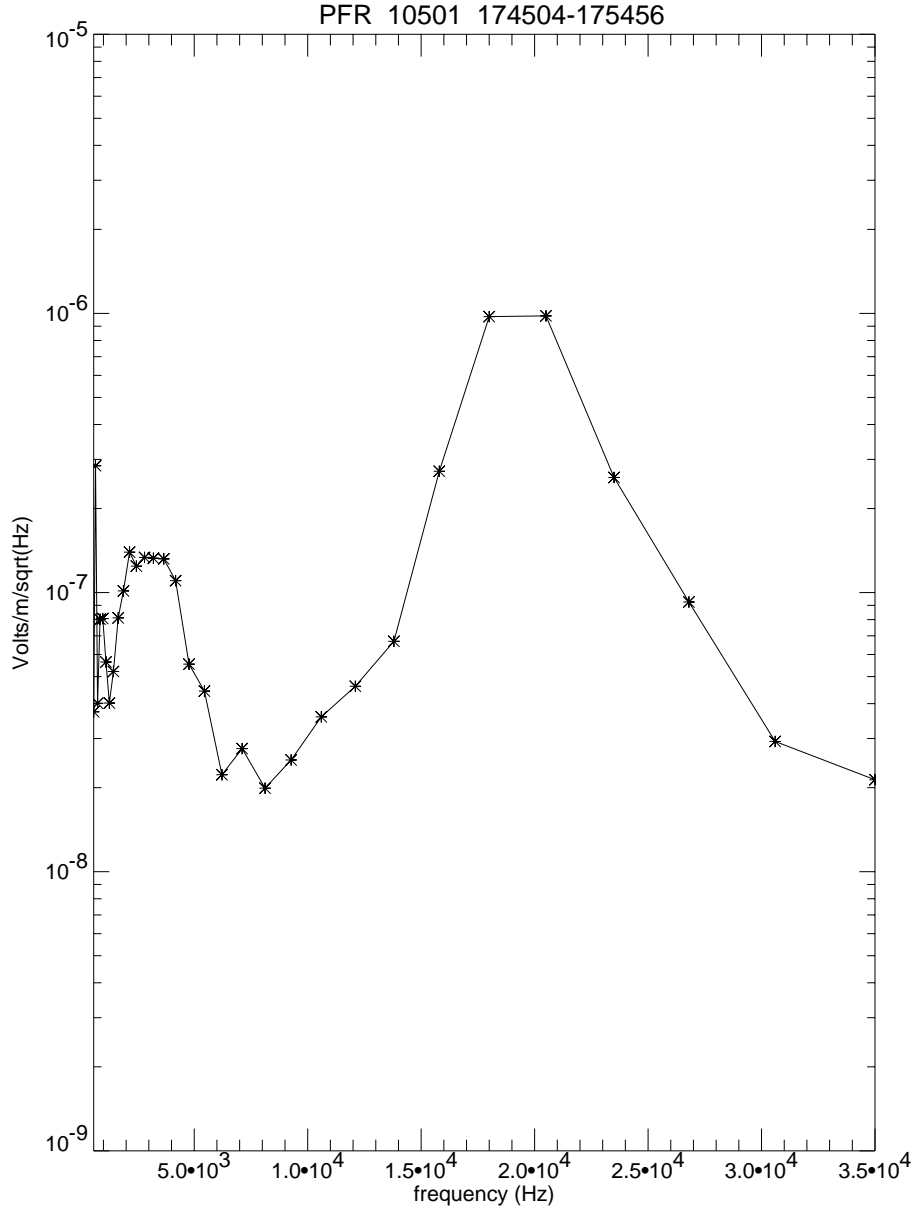


Fig. 3. The average spectra of the wave electric field signals obtained by the plasma frequency receiver (PFR) in the interval 17:45:04–17:54:56 UT. The spectral peaks at ~ 3 kHz and ~ 20 kHz correspond to the high frequency ion sound and Langmuir waves, respectively.

The damping rate of the ion sound waves which depends on electron to ion temperature ratio (T_e/T_i) as

$$\frac{\Gamma_s}{\omega_s} \sim \sqrt{\frac{\pi}{2}} \left[0.32 \frac{T_e}{T_i} \exp\left(\frac{-T_e}{2T_i}\right) + \left(\frac{m_e}{m_i}\right)^{\frac{1}{2}} \right], \quad (3)$$

is $\simeq 0.25$ for the observed $T_e \simeq 1.7 \times 10^5$ K, and $T_i \simeq 4.9 \times 10^4$ K. The relative energy density of these waves

$$\frac{W_s}{n_e T_e} \sim \frac{\epsilon_0 E_s^2}{n_e T_e}, \quad (4)$$

is $\sim 10^{-9}$ for $\epsilon_0 = 8.85 \times 10^{-12}$ Fm $^{-1}$, $E_s \sim 10^{-4}$ Vm $^{-1}$, $n_e = 4.5$ cm $^{-3}$ and $T_e = 1.7 \times 10^5$ K.

The dispersion relation of Langmuir waves is

$$f_L = f_{pe} \left(1 + \frac{3k_L^2 \lambda_D^2}{2} \right), \quad (5)$$

where

$$k_L = \frac{2\pi f_{pe}}{v_b}, \quad (6)$$

for the beam-excited Langmuir waves. Ulysses was located at a distance of 1.36 AU from the Sun during this event. By using the $1/f$ plot of the type III burst, we estimate the beam speed v_b as $\sim 3 \times 10^9$ cms $^{-1}$,

and $k_L = 2\pi f_{pe}/v_b \sim 4.0 \times 10^{-5} \text{ cm}^{-1}$ for $f_{pe} = 19 \text{ kHz}$. The damping rate of Langmuir waves

$$\frac{\Gamma_L}{\omega_{pe}} \sim \sqrt{\frac{\pi}{2}} \left(\frac{n_b}{n_e}\right) \left(\frac{v_b}{\Delta v_b}\right)^2, \quad (7)$$

is $\sim 1.2 \times 10^{-5}$ for $\Delta v_b/v_b \simeq 0.1$ and $n_b/n_e \simeq 10^{-7}$, where n_b and n_e are the electron density in the beam and ambient plasma, and v_b , and Δv_b are the beam speed and its dispersion.

The peak amplitudes and spatial scales of the coherent electric field structures of Langmuir waves are important signatures of the nonlinear processes. The FES records intense plasma wave activity with a time resolution of up to 1 ms per data sample, and a total of 1024 contiguous samples are recorded for an event. The most intense event observed during an interval of approximately one-half hour is telemetered. Electric field measurements are made over a wide-frequency band determined by commandable filters, each having a range of one decade in frequency, e.g. 6–60 kHz and 2–20 kHz.

Figure 4 presents two Langmuir wave envelopes captured by the low frequency band of FES on 1 May 2001 at 17:53:53 and 18:19:29 UT. These events are associated with the local type III radio burst of $\sim 16:00$ – $18:00$ UT (Fig. 1). As seen from Fig. 4, the Langmuir wave envelopes show a broad intense peak after ~ 500 ms. The fluctuations seen in the beginning phase of these events are probably due to low frequency waves such as the long wavelength ion sound waves. The asymmetric shapes of these events are due to the 32-dB attenuator activated by the intense central peak. The role of the attenuator is to extend the dynamic range of the system, i.e. whenever the signal rises to saturation, the attenuator is switched into the signal stream and remains connected for the remainder of the event cycle. The millisecond spikes on the broad intense peaks are transients associated with the activation of the attenuator.

The peak electric fields E_L of these broad peaks are $\sim 5 \times 10^{-3}$ and $3 \times 10^{-3} \text{ V/m}$, and the corresponding $W_L/(n_e T_e) = \epsilon_0 E_L^2 / (n_e T_e)$ are 2×10^{-5} and 2×10^{-6} , respectively, for $n_e = 4.5 \text{ cm}^{-3}$ and $T_e = 1.7 \times 10^5 \text{ K}$. The half-power duration (T) of the broad central peaks of these events are less than or equal to 10 ms. Because these field structures are convected by the solar wind, their spatial scales $L = T v_{sw}$ are $\leq 300 \lambda_D \sim 4 \text{ km}$ for $v_{sw} \sim 365 \text{ km s}^{-1}$. These spatial scales are of the order of the wavelengths of Langmuir waves, indicating that they are probably undergoing self-focussing and related nonlinear processes. Table 1 summarizes the observed parameters of Langmuir and ion sound waves, and other solar wind parameters.

3 Discussion

The electrostatic decay instability is believed to be responsible for the low-frequency electrostatic waves observed in association with Langmuir waves in type III burst source regions (Lin et al., 1986) as well as in the Earth's electron

foreshock region (Anderson et al., 1981) (the low-frequency electrostatic waves were interpreted in terms of the daughter products of the electrostatic decay of the beam-excited Langmuir waves). The threshold for this instability is given by

$$\frac{W_{th}}{n_e T_e} = \frac{4\Gamma_L \Gamma_s}{\omega_s \omega_{pe}}. \quad (8)$$

In the present case, this threshold is $\sim 10^{-5}$ for the damping rates of $\Gamma_s/\omega_s \simeq 0.25$ and $\Gamma_L/\omega_{pe} \sim 1.2 \times 10^{-5}$ (Eqs. 3 and 7). On the other hand, the observed $\frac{W_L}{n_e T_e}$ values range from 2×10^{-6} to 2.0×10^{-5} (see Table 1). Even though the threshold condition is satisfied in the present case, the electrostatic decay instability does not occur unless the Langmuir and ion sound waves satisfy the relevant resonance conditions, which impose a constraint $k_s \leq 2k_L - k_0$ (Thejappa et al., 2003), where $k_0 \sim 2\omega_{pe} v_s / 3v_{Te}^2 \sim 1.2 \times 10^{-5} \text{ cm}^{-1}$, for $f_{pe} \sim 19 \text{ kHz}$, ion-sound speed, $v_s = \sqrt{T_e/m_i} \sim 3.8 \times 10^6 \text{ cm s}^{-1}$ and the electron thermal speed, $v_{Te} = \sqrt{T_e/m_e} \sim 1.6 \times 10^8 \text{ cm s}^{-1}$. This constraint provides the upper limit on the wave numbers and frequencies of the ion sound waves, which could be produced by electrostatic decay instability. These are $k_s \sim 6.8 \times 10^{-5} \text{ cm}^{-1}$, $f_s = k_s v_s / 2\pi \sim 41 \text{ Hz}$ for $k_L \sim 4.0 \times 10^{-5} \text{ cm}^{-1}$ and $k_0 \sim 1.2 \times 10^{-5} \text{ cm}^{-1}$. These k_s values also provide the highest possible doppler shift $k_s v_{sw} / (2\pi)$ as $\sim 393 \text{ Hz}$ for v_{sw} of 365 km s^{-1} . Therefore, if the ion sound waves are excited by the electrostatic decay instability, their frequencies should be $\leq 434 \text{ Hz}$, i.e. well below the observed frequencies of 2–4 kHz. Thus, the electrostatic decay instability is probably not responsible for the observed short wavelength ion sound waves.

The short wavelength ion sound waves can also be excited by the thermalization of the empty burnt-out cavitons left behind by the Langmuir collapse (Galeev et al., 1976). Goldman and Nicholson (1978) have derived an expression for the threshold for the collapse of a two-dimensional Langmuir wave packet using the virial theorem. According to these authors the threshold condition for Langmuir collapse is:

$$\frac{W_{th}}{n_e T_e} = 24(\Delta k_L \lambda_D)^2, \quad (9)$$

where Δk_L is the half-width of the Langmuir wave packet. Melrose and Goldman (1987) applied this threshold condition to interpret the observations reported by Lin et al. (1986). These authors estimate the spread in wave numbers as:

$$\frac{\Delta k_L}{k_L} \sim \frac{\Delta v_b \ln 2}{v_b 2N}, \quad (10)$$

where N is the number of linear growth times before the onset of saturation mechanism. In the present case, we can use the Eqs. (9) and (10) to estimate the threshold as follows. The number of linear growth times N can be written as $\sim \ln p \sim 7$, where $p \simeq 10^3$ (cf. Fig. 4) is the observed ratio of the peak electric field amplitude to the instrumental background. Therefore, for $\Delta v_b/v_b \sim 0.15$, and $N \sim 7$, we obtain $\Delta k_L/k_L \sim 7 \times 10^{-3}$ and $\frac{W_{th}}{n_e T_e} \sim 3 \times 10^{-6}$ for $\lambda_D \sim 13.6 \text{ m}$ and

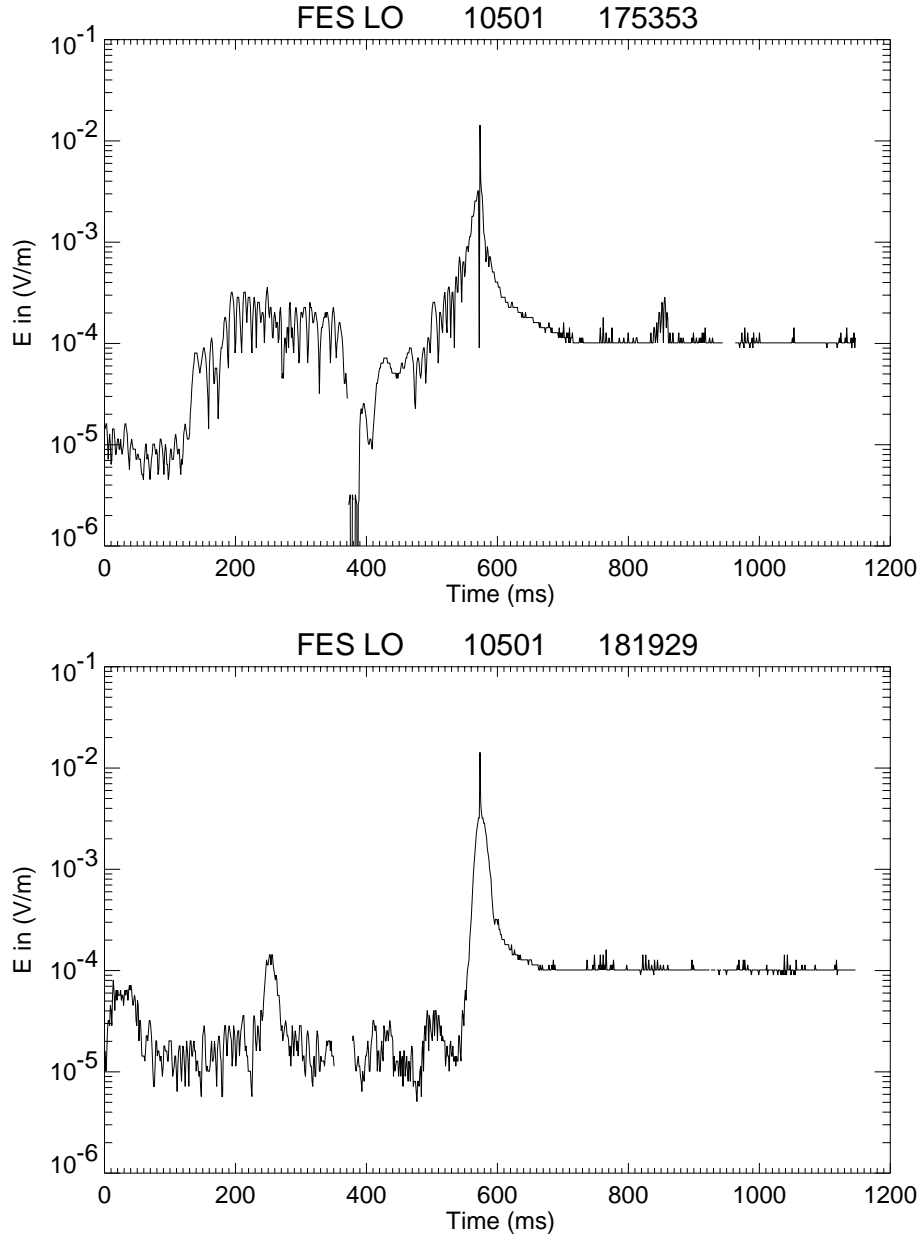


Fig. 4. FES events corresponding to Langmuir waves of the local type III burst of 16:00 UT (Fig. 1). Millisecond spikes are transients due to the finite time response during the attenuator activation.

$k_L = 4 \times 10^{-3} \text{ m}^{-1}$. This threshold value is comparable to the observed values of $\frac{W_L}{n_e T_e}$ of $\sim 2 \times 10^{-5}$ and 8×10^{-6} (see, Table 1). These observations are consistent with the theoretical and computational results for the evolution of beam excited Langmuir waves (Goldman and Nicholson, 1978; Nicholson et al., 1978). As far as the recent hypotheses of Langmuir collapse based on the localized Langmuir eigenstates in the ocean of plane waves as seen in numerical simulations are concerned (Robinson, 1997), there is no observational evidence for structures with $f < f_{pe}$. A detailed analysis of WIND data of Langmuir wave spectra and high time resolution electron data will be able to confirm the related nucleation mechanism of Langmuir collapse.

The wavelengths of ion-acoustic waves generated during the relaxation of burnt-out cavitons should be of the order of the spatial scales of collapsing structures $\sim 15\lambda_D$. Accordingly, the wavenumbers of these waves k_s are $\sim 3.4 \times 10^{-2} \text{ m}^{-1}$. For such waves, the frequency is mostly determined by the Doppler shift of these waves by the solar wind, which can be estimated as $k_s v_{sw} \sim 2 \text{ kHz}$ for the solar wind speed of $v_{sw} \sim 365 \text{ km s}^{-1}$. These frequencies agree very well with the observed short wavelength ion sound waves.

Table 1. The physical parameters.

Parameters	Values
INTERPLANETARY PLASMA	
Electron density, n_e	4.5 cm^{-3}
Electron temperature, T_e	$1.74 \times 10^5 \text{ K}$
Ion temperature, T_i	$4.9 \times 10^4 \text{ K}$
Debye length, λ_D	$1.36 \times 10^3 \text{ cm}$
Electron plasma frequency, f_{pe}	19 kHz
Solar wind velocity, v_{sw}	365 km s^{-1}
Electron thermal speed, V_{Te}	$1.6 \times 10^8 \text{ cm s}^{-1}$
Ion thermal speed, V_{Ti}	$2.0 \times 10^6 \text{ cm s}^{-1}$
Ion acoustic speed, c_s	$3.8 \times 10^6 \text{ cm s}^{-1}$
Ambient magnetic field (B)	5.3 nT
Electron Cyclotron Frequency	150 Hz
$\frac{f_{ce}}{f_{pe}}$	7.8×10^{-3}
LANGMUIR WAVES	
Beam excited Langmuir wave number, k_L	$4.0 \times 10^{-5} \text{ cm}^{-1}$
Relative Peak Energy density, $\frac{W_L}{n_e T_e}$	$2 \times 10^{-6} - 2 \times 10^{-5}$
The wavelength of Langmuir waves, $\lambda_0 \sim 2\pi/k_L$	3.1 kms
ION SOUND WAVES	
The peak electric field, E_s at 2 kHz	$\sim 10^{-4} \text{ V/m}$
Relative Energy Density, $\frac{W_s}{n_e T_e}$	$\sim 10^{-8}$

The emissivity of the short wavelength ion sound waves excited by the burnt-out cavitons can be written as (Galeev et al., 1976)

$$\alpha = 2\gamma_M W_L^* k_L^2 \lambda_D^2. \quad (11)$$

Here

$$\gamma_M = \omega_{pe} \sqrt{m_e/m_i} \left(\frac{W_L}{n_e T_e}\right)^{1/2} \quad (12)$$

is the growth rate of the modulational instability, and

$$W_L^* = W_L \left(\frac{k_0}{k_L}\right)^{3/2} \quad (13)$$

is the energy in the short wave part of the Langmuir wave spectrum in 3-dimensions, and

$$k_0 = \frac{1}{\lambda_D} \sqrt{\frac{W_L}{n_e T_e}} \quad (14)$$

is the wave number at which energy is pumped into the Langmuir waves.

The absorption of the ion-sound waves by the background electrons is given by

$$\gamma_s = \omega_{pe} \frac{m_e}{m_i} k_L \lambda_D. \quad (15)$$

In a steady state, the emissivity is equal to the absorption, i.e., one can write

$$2\gamma_M W_L^* k_L^2 \lambda_D^2 = 2\gamma_s W_s. \quad (16)$$

This in turn gives the energy density of the emitted ion sound waves as

$$\frac{W_s}{n_e T_e} = \sqrt{\frac{m_i}{m_e k_L \lambda_D}} \left(\frac{W_L}{n_e T_e}\right)^{9/4}, \quad (17)$$

which can be estimated as $\simeq 10^{-8}$ for the observed values of $W_L/(n_e T_e) \sim 2 \times 10^{-5}$, $k_L \sim 4.0 \times 10^{-5} \text{ cm}^{-1}$ and $\lambda_D \sim 13.5 \times 10^2 \text{ cm}$. This value agrees reasonably well with the observed energy density of $\sim 3.7 \times 10^{-8}$.

While deriving the threshold condition (9) Goldman and Nicholson (1978) have assumed the condition

$$\frac{9}{2} k_0^2 \lambda_D^2 \ll \frac{m_e}{m_i} \quad (18)$$

is satisfied, i.e. adiabatic ion approximation. For the wave numbers k_L obtained using the beam speeds derived from the frequency drift of type III bursts, the above inequality is not satisfied. Most probably, some nonlinear process such as induced scattering of Langmuir waves off thermal ions pumps them to lower wave numbers k_0 where the above condition is satisfied.

4 Conclusions

We summarize the results of this study as follows: (1) The Ulysses/URAP experiment has observed a number of local type III bursts excited in the vicinity of the spacecraft. (2) The high resolution observations of the Langmuir

waves associated with these type III events indicate that the Langmuir wave packets occur as highly structured intense wave packets with half-power duration of 10's of milliseconds which are equivalent to a few hundred Debye lengths. The relative peak energy density of these Langmuir waves, $W_L/n_e T_e$ is $\sim 10^{-5}$. (3) Short wavelength ion sound waves in the 2–4 kHz range sometimes occur in association with these strongly turbulent Langmuir waves, (4) The threshold for electrostatic decay is $\sim 8 \times 10^{-8}$ which is much less than the observed values of $W_L/n_e T_e$. However, the predicted frequencies of ion-acoustic waves due to electrostatic decay are ≤ 450 Hz (including the contribution of the doppler shift in the solar wind). No electric field signals are observed at these frequencies. (5) The observed high frequency ion sound waves in close association with Langmuir waves are not due to electrostatic decay because neither their frequencies nor their wavelengths satisfy the required resonance conditions. (6) The peak intensities of the Langmuir wave field structures captured by the high resolution FES are of the order of the thresholds for direct Langmuir collapse, and their spatial scales are of hundreds of Debyelengths indicating that these structures are probably in the state of strong turbulence. (7) The wavelengths of observed high frequency ion sound waves are comparable to the spatial scales of the collapsing Langmuir wave field structures. (8) The observed short wavelength ion sound waves are most probably emitted by the empty burnt out cavitons left behind by the Langmuir collapse processes. (9) The peak intensity of the observed high frequency ion sound waves are comparable to the predicted values of ion sound waves radiated by the burnt out cavitons where the observed parameters of Langmuir waves were used. (10) However, the speeds of the electron beams derived from the frequency drift of type III radio bursts are too slow to satisfy the needed adiabatic ion approximation. Therefore, some non-linear process such as the induced scattering on thermal ions most probably pumps the beam excited Langmuir waves towards the lower wavenumbers, where the adiabatic ion approximation is justified.

Acknowledgements. The URAP investigation is a collaboration of NASA Goddard Space Flight Center, the Observatoire de Paris-Meudon, the University of Minnesota and the Centre d'études des Environnements Terrestre et Planétaires (CETP). The research of GT is supported by the NASA grant NCC-255. Solar wind data from the Ulysses SWOOPS instrument were obtained from the NSSDC.

Edited by: G. S. Lakhina

Reviewed by: P. J. Kellogg and another referee

References

- Anderson, R. R., Parks, G. K., Eastman, T. E., Gurnett, D. A., and Frank, L. A.: Plasma-waves associated with energetic particles streaming into the solar-wind from the earth's bow shock, *J. Geophys. Res.*, 86, 4493–4510, 1981.
- Bame, S. J. et al.: The Ulysses solar wind plasma experiment, *Astron. Astrophys. Suppl. Ser.*, 92, 237–265, 1992.
- Burmasov, V. S., Vyacheslavov, L. N., Kandaurov, I. V., Kruglyakov, E. P., Meshkov, O. I., and Sanin, A. L.: Excitation of ion-sound fluctuations in a magnetized plasma with strong Langmuir turbulence, *Plasma Phys. Rep.*, 23, 126–129, 1997.
- Cheung, P. Y., and Wong, A. Y.: Nonlinear evolution of electron-beam plasma interactions, *Phys. Fluids.*, 28, 1538–1548, 1985.
- Degtyarev, L. M., Sagdeev, R. Z., Solov'ev, G. I., Shapiro, V. D., and Shevchenko, V. I.: One-dimensional Langmuir turbulence, *Sov. J. Plasma Phys.*, 6, 263, 1980.
- Do Prado, F., Karfidov, D. M., Alves, M. V., and Dallaqua, R. S.: Ion sound wave excitation in a plasma under a strong Langmuir turbulence regime, *Phys. Lett. A.*, 248, 86–91, 1998.
- Doolen, G. D., DuBois, D. F., and Rose, H. A.: Nucleation of cavitons in strong Langmuir turbulence, *Phys. Rev. Lett.*, 54, 804–807, 1985.
- DuBois, D. F., Hanssen, A., Rose, H. A., and Russell, D.: Space and time distribution of HF excited Langmuir turbulence in the ionosphere – comparison of theory and experiment, *J. Geophys. Res.*, 98, 17 543–17 567, 1993.
- Galeev, A. A., Sagdeev, R. Z., Shapiro, V. D., and Shevchenko, V. I.: Effect of acoustic turbulence on the collapse of Langmuir waves, *JETP Lett.*, 24, 21–24, 1976.
- Goldman, M. V., and Nicholson, D. R.: Virial theory of direct Langmuir collapse, *Phys. Rev. Lett.*, 41, 406–410, 1978.
- Goldman, M. V.: Strong turbulence of plasma waves, *Rev. Mod. Phys.*, 56, 709–735, 1984.
- Goldstein, M. L., Smith, R. A. and Papadopoulos, K.: Nonlinear stability of solar type III radio bursts, II. Application to observations near 1 AU, *Astrophys. J.*, 237, 683–695, 1979.
- Gurnett, D. A., Maggs, J. E., Gallagher, D. L., Kurth, W. S., and Scarf, F. L.: Parametric interaction and spatial collapse of beam-driven Langmuir waves in the solar wind, *J. Geophys. Res.*, 86, 8833–8841, 1981.
- Gurnett, D. A., Hospodarsky, G. B., Kurth, W. S., Williams, D. J., and Bolton, S. J.: Fine structure of Langmuir waves produced by a solar electron event, *J. Geophys. Res.*, 98, 5631–5637, 1993.
- Karfidov, D. M., Rubenchik, A. M., Sergeichev, K. F., and Sychov, I. A.: Strong Langmuir turbulence excited in a plasma by an electron beam, *JETP*, 98, 1592–1604, 1990.
- Karfidov, D. M., and Lukina, N. A.: Electrical fields in a plasma with strong Langmuir turbulence, *Phys. Lett. A.*, 232, 443–446, 1997.
- Kellogg, P. J., Goetz, K., Howard, R. L. and Monson, S.: Evidence for Langmuir wave collapse in the interplanetary plasma, *Geophys. Res. Lett.*, 19, 1303–1306, 1992a.
- Kellogg, P. J., Goetz, K., Lin, N., Monson, S., Balogh, A., Forsyth, R. J., and Stone, R. G.: Low frequency magnetic signals associated with Langmuir waves, *Geophys. Res. Lett.*, 19, 1299–1302, 1992b.
- Kellogg, P. J., Goetz, K., Monson, S. J., and Bale, S. D.: A search for Langmuir solitons in the Earth's foreshock, *J. Geophys. Res.*, 104, 6751–6757, 1999.

- Lin, R. P., Levedahl, W. K., Lotko, W., Gurnett, D. A. and Scarf, F. L.: Evidence for nonlinear wave-wave interactions in solar type III radio bursts, *Astrophys. J.*, 308, 954–965, 1986.
- McFarland, M. D., and Wong, A. Y.: Spectral content of strong Langmuir turbulence in the beam plasma interaction, *Phys. Plasmas*, 4, 945–955, 1997.
- Melrose, D. B. and Goldman, M. V.: Microstructures in type III events in the solar wind, *Solar Phys.*, 107, 329–350, 1987.
- Meyer-Vernet, N., and Perche, C.: Tool kit for antennae and thermal noise near the plasma frequency, *J. Geophys. Res.*, 94, 2405–2415, 1989.
- Montgomery D. S., Johnson, R. P., Cobble, J. A., Fernandez, J. C., Lindman, E. L., Rose, H. A., and Estabrook, K. G.: Characterization of plasma and laser conditions for single hot spot experiments, *Laser and Particle Beams*, 17, 349–359, 1999.
- Nicholson, D. R., Goldman, M. V., Hoyang, P. and Weatherall, J. C.: Nonlinear Langmuir waves during type III solar radio bursts, *Astrophys. J.*, 223, 605–619, 1978.
- Papadopoulos, K., Goldstein, M. L. and Smith, R. A., Stabilization of electron streams in type III solar radio bursts, *Astrophys. J.*, 190, 175–185, 1974.
- Pelletier, G.: Generation of a high-energy electron tail by strong Langmuir turbulence in a plasma, *Phys. Rev. Lett.*, 49, 782–785, 1982.
- Pelletier, G., Sol, H., and Asseo, E.: Magnetized Langmuir wave packets excited by a strong beam plasma interaction, *Phys. Rev.*, 38, 2552–2563, 1988.
- Reiner, M. J., Fainberg, J. and Stone, R. G.: Detection of fundamental and harmonic type III radio emission and associated Langmuir waves at the source region, *Astrophys. J.*, 394, 340–350, 1992.
- Robinson, P. A.: Nonlinear wave collapse and strong turbulence, *Rev. Mod. Phys.*, 69, 507–573, 1997.
- Smith, R. A., Goldstein, M. L. and Papadopoulos, K., Nonlinear stability of solar type III radio bursts, I. Theory, *Astrophys. J.*, 234, 348–362, 1979.
- Stone, R. G., et al.: The Unified radio and plasma wave investigation, *Astron. Astrophys. Suppl. Ser.*, 92, 291–316, 1992.
- Thejappa, G., Lengyel-Frey, D., Stone, R. G. and Goldstein, M. L., Evaluation of emission mechanisms at ω_{pe} using Ulysses observations of type III bursts, *Astrophys. J.*, 416, 831–844, 1993.
- Thejappa, G., Wentzel, D and Stone, R. G.: Low-frequency waves associated with Langmuir waves in solar wind, *J. Geophys. Res.*, 100, 3417–3426, 1995b.
- Thejappa, G., R. G. Stone and M. L. Goldstein, Detection of Langmuir solitons: Implications for type III burst emission mechanisms at $2\omega_{pe}$, *Astrophysics and space sci.*, 243, 195–198, 1996.
- Thejappa, G., and MacDowall, R. J.: Evidence for strong and weak turbulence processes in the source region of a local type III radio burst, *Astrophys. Jou.*, 498, 465–478, 1998.
- Thejappa, G., Goldstein, M. L., MacDowall, R. J., Papadopoulos, K., and Stone, R. G.: Evidence for Langmuir envelope solitons in solar type III burst source regions, *J. Geophys. Res.*, 104, 28 279–28 293, 1999.
- Thejappa, G., MacDowall, R. J., Scime, E. E., and Littleton, J. E., Evidence for electrostatic decay in the solar wind at 5.2 AU, *J. Geophys. Res.*, 108, A3, Art. No. 1139, doi:10.1029/2002JA009290, 2003.
- Thiessen, J. P., and Kellogg, P. J.: Langmuir wave decay and collapse in the jovian foreshock, *Pla. Spa. Sci.*, 41, 823–832, 1993.
- Vyacheslavov, L. N., Burmasov, V. S., Kandaurov, I. V., Kruglyakov, E. P., Meshkov, O. I., and Sanin, A. I.: Dissipation of strong Langmuir turbulence in nonisothermal non-Maxwellian plasma, *JETP Lett.*, 75, 41–54, 2002.
- Zakharov, V. E., Collapse of Langmuir waves, *Sov. Phys. JETP*, 35, 908–914, 1972.